Ray Tracing Simulations of Indoor Channel Spatial Correlation for Physical Layer Security

Enrico M. Vitucci[1], Francesco Mani[2], Taghrid Mazloum[2], Alain Sibille[2], Vittorio degli Esposti[1]
[1]Dipartimento di Ingegneria dell'Energia Elettrica e dell'Informazione Guglielmo Marconi (DEI),
University of Bologna, Cesena, Italy
[2]Communication and Electronic Department, Telecom ParisTech/LTCI, Paris, France

***Abstract*—The goal of this work is to establish the accuracy of ray tracing to simulate the radio channel in a Physical Layer Security scenario, where two legitimate users try to take advantage of the intrinsic properties of the channel to generate a shared secret key inaccessible to an eavesdropper. A 3D Ray-Tracing software, including a diffuse scattering model, is employed to simulate spatial correlations in an indoor environment at the frequencies of 2.4 and 5GHz. Measurements, performed with a Vector Network Analyzer, are used to assess the validity of simulated results.**

***Index Terms*—Physical layer security, propagation, ray-tracing, indoor radio communications.**

I. Introduction

Wireless communications are nowadays ubiquitous and they play an important role in many fields of society, therefore one of their crucial requirement is security. The public nature of wireless communications puts them in danger towards the possibility of an eavesdropper (classically referred to as Eve) to access the information exchanged between the legitimate users (identified as Alice and Bob). Fig.1 exemplifies this scenario.

Secret keys may be used to encrypt data to ensure the confidentiality of the communication. Although conventional cryptographic security mechanisms are widely used to generate such keys, recently new approaches have been investigated in order to take profit from the physical layer properties of the communication channel.

Physical layer security (PhySec) is the ensemble of techniques that exploits the inherent properties of the propagation channel, e.g. noise, interference, and the time-varying nature of fading channels, to establish a secure connection. In this work we specifically focus on the topic of PhySec that studies the generation of secure keys from the time-varying channel coefficients. Following the law of reciprocity, the forward and reverse propagation channel between Alice and Bob are ideally identical and in practice very similar. Therefore, it is safe to assume that with an adequate algorithm it is possible for Alice and Bob to generate a common secret key exploiting the shared randomness of the reciprocal time-varying channel. Moreover, in a rich multipath environment, fast fading creates significant spatial decorrelation so that Eve experiences completely different channel time variations and, accordingly, it is not able to correctly reconstruct the key generated by the legitimate users.

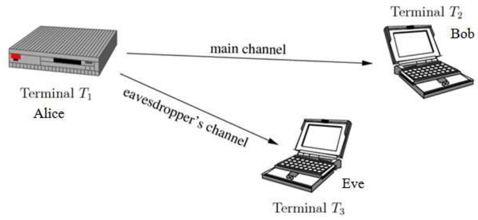

Fig. 1. PhySec communication scenario

In literature, it is possible to find many examples of measured channels used to test key generation algorithms or to validate information theory based channel security performances [1]–[3]. But, it is well known that measurements are costly, time-consuming and not always possible to be performed. Ray-Tracing (RT) is a powerful technique that enables to generate accurate channel characteristics in site-specific scenarios. Despite being widely used in many wireless application scenarios to predict channel behavior [4]–[7], very few examples of RT to create channel coefficients to study PhySec can be found [8]. The goal of this preliminary work is to validate with channel measurements in an indoor environment the ability of RT simulations to accurately predict the spatial decorrelation between a legitimate user and Eve from a statistical point of view.

II. Measurement Description

Measurements have been carried out on a floor with classrooms and offices in Telecom ParisTech building on a school holiday so that no-one was moving in and around the environment during measurement time. They have been recorded with a 4-port vector network analyzer (VNA) with the setup parameters presented in Table I. The four ports have been devoted in the following way: one for Alice, one for Bob and two for Eve. Each port was equipped with an identical UWB bicone antenna, which description can be found in [9].

The terminal representing Alice has been automatically positioned on a square grid of 121 points with 30 cm side and 3 cm step. The grid has been scanned with a rotating positioner mounted on top of a linear rail. The antenna was placed on a mast displaced by a radius $\rho = 25\ cm$ from the center of the rotating motor. The Cartesian position (x_i, y_i) of Alice has been mapped to the polar coordinates (r_i, ψ_i),

TABLE I
VNA SETUP PARAMETERS

Start frequency	2 GHz
Stop frequency	6 GHz
Bandwidth	4 GHz
Transmitted power	10 dBm
Frequency points	1601
IF Bandwidth	5kHz
AVG Factor	1

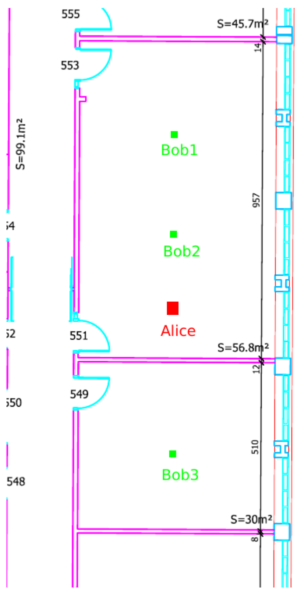

Fig. 2. Map of the measurement scenario

where r_i represents the position on the rail and ψ_i the angle of the rotating motor, in the following way:

$$\begin{cases} r_i = x_i - \rho\cos(\psi_i) \\ \psi_i = \arcsin(y_i/\rho) \end{cases} \tag{1}$$

The positioning devices and the VNA were controlled through GPIB connections with a MATLAB script. A pause of 5 s has been programmed after each movement of the rotating motor to let the mast stabilize before performing the measurement.

Three positions of the terminal representing Bob have been set as depicted in Fig.2, i.e. two in the same room of Alice and one in the next room. Finally, for each Bob position, eight couple of positions are set for the two Eve terminals for a total of 16 Eve positions, displaced in the two rooms and in the corridor at different distances from Bob. All the antennas were positioned at a height of 1.3 m from the ground.

RT simulations are, in principle, noise free. Normally this should be taken into account for comparison with measurements. In this case, however, the Signal-to-Noise Ratio (SNR) recorded in the measurements is sufficiently high, i.e. $SNR \approx 40\ dB$, for them to be considered noise free.

III. Ray Tracing Model

The RT software used in this work [10] is a full (3D) model that relies upon the full geometrical description of the propagation environment, including walls and objects. 3D polarimetric radiation properties of the antennas and electromagnetic properties of the materials at different frequencies are also taken into account.

A maximum number of 3 reflections and single diffraction are considered for each ray in the simulations. Combinations of reflections and diffraction in the same ray are allowed. A maximum of ten transmissions is also set for each ray, in order to neglect rays which do not carry significant power. Diffuse scattering is included using a model based on the Effective Roughness (ER) approach [11]. Each surface is divided in surface elements. Each of those generates a scattering ray whose amplitude depends on a scattering coefficient S and on a directive scattering pattern, centered around the direction of specular reflection.

This scattering diagram can be then expressed as:

$$Es(r_s, \theta_s, \phi_s) = E_{s0}\left(\frac{1+\cos\psi_R}{2}\right)^{\frac{\alpha_R}{2}} \tag{2}$$

where E_{s0} depends on the scattering coefficient S that sets the amount of scattered power, ψ_R is the angle between the direction of the specular reflection and the scattering direction (θ_s, ϕ_s), and the exponent α_R sets the width of the scattering lobe [11].

In the simulations, single bounce scattering with values of $S = 0.5$ and $\alpha_r = 2$ is considered, in accordance to what found in previous works where the model has been parametrized in indoor environments [12]. The ER model in its original formulation assumes that diffuse scattering is totally incoherent, i.e. only the amplitude of the diffuse field is modeled. Nevertheless, in this work we are interested in reproducing the complex channel coefficients. Therefore, we need to generate a phase associated with the aforementioned amplitude. As preliminary approach, random phases with a uniform distribution over $[0, 2\pi]$ are associated with scattered rays. This may result in a simplistic approach as, intuitively, rays scattered by neighboring surface elements should have a correlated phase.

IV. Simulation Results and Comparison with Measurements

RT simulations are run at the frequencies of 2.4 and 5 GHz and comparison with measurements are shown in this section. Such frequencies have been selected for the study within the measurement band, being of particular interest because they are both used in WiFi.

A simplified environment description is adopted in the RT input database. The walls, ceiling and floor of the two rooms and the corridor where the terminals were placed (see Fig. 2) are obviously included. In addition, doors and windows are also modeled together with a metalized whiteboard on the wall separating the two rooms that plays an important

TABLE II
MEAN ABSOLUTE ERROR AND ERROR STANDARD DEVIATION OF PREDICTED POWER

Freq. (GHz)	Mean abs. error (dB)	Error std. dev. (dB)
2.4	2.1	1.7
5.0	1.6	1.3

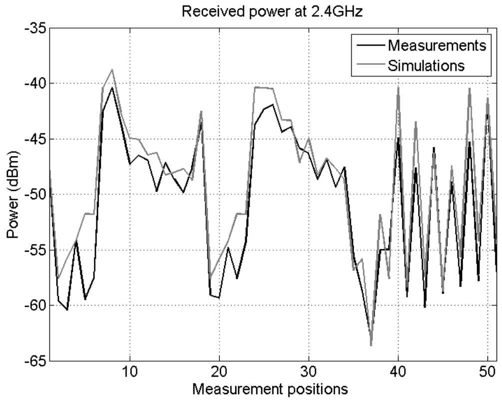

Fig. 3. Comparison of the Received Power at 2.4 GHz

role when room to room propagation is occurring. Tables, chairs and other small objects are not taken into account in the simulations.

A. Validation of RT Via Received Power Comparison

A first validation of the RT model in the considered scenario has been done through comparisons of the predicted narrowband powers with respect to the measurements. All the channels between Alice and Bob/Eve are considered, with a total of $3 + 3 \times 16 = 51$ receiving points. Such comparison is reported in Fig.3 for the 2.4 GHz frequency, which shows a very good agreement. The agreement is even better at 5 GHz, so the corresponding figure is not shown here for brevity. It is worth considering however that the curves of Fig.3 show local averages for different, non adjacent receiving positions, and therefore don't include fast fading prediction inaccuracies, which have been averaged out. In Table II, the mean absolute values and the standard deviations of the errors with respect to the measurements are shown for both frequencies.

B. Bob-Eve Correlation

The crucial channel parameter that defines PhySec performances is the correlation between the channel seen by the legitimate users and the one seen by the eavesdropper. In this section, we try to verify the ability of RT to predict correlations of the channel amplitudes. The correlation coefficient $\rho_{X,Y}$ between the two vectors X and Y is defined as:

$$\rho_{X,Y} = \frac{E[(X - \mu_X)(Y - \mu_Y)]}{\sigma_X \sigma_Y} \tag{3}$$

where μ stands for the mean and σ is the standard deviation. Here, the statistical set over which the correlation is evaluated is formed by the different positions of Alice in the grid.

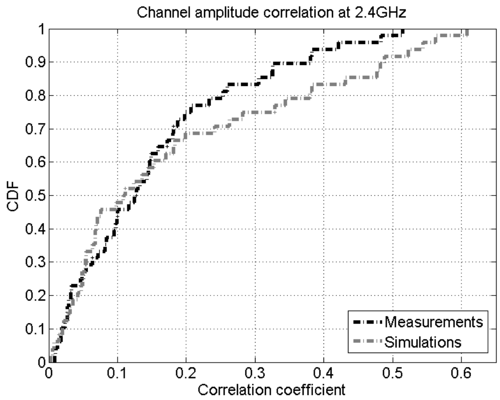

Fig. 4. CDF of correlation coefficient of channel amplitudes seen by Bob and Eve at 2.4 GHz

Therefore, the two vectors have as elements the channel coefficients seen by Bob and Eve with respect to Alice. Then, the legitimate channels are $h_{BA} = [h_{b1}, ..., h_{bn}, ..., h_{b121}]$, with n being the index of Alice position, while the illegitimate ones are $h_{EA} = [h_{e1}, ..., h_{en}, ..., h_{e121}]$. The Cumulative Distribution Functions (CDFs) of the amplitude correlation coefficients between the channels seen by Bob and Eve are shown in Fig.4 and Fig.5 for the 2.4 and 5 GHz frequencies, respectively. To reduce the number of figures, results from different Bob positions are aggregated in the same figure. The agreement is fairly good, since both the average value and the distribution are quite well reproduced by the RT simulations. The slightly lower correlation of the simulated channel seems to suggest that the totally random phase for the diffuse component is probably too strong as assumption. Analyzing the figure, we can see that measured results show a very low correlation between Bob and Eve channels. This could be expected since the smaller distance between the two is 44 cm that is larger than 3.5λ and 7λ at 2.4 GHz and 5 GHz, respectively. Therefore we can expect key generated from channel amplitudes to be highly secure.

It is interesting to note that RT simulations are able to predict quite well the decorrelation between the channels seen by the two terminals from a statistical point of view. However, it has to be noticed that this accuracy is achieved with an accurate, although simplified, description of the environment together with the precise position of the terminals. Therefore, RT cannot be easily used by Eve as a tool to violate the security of the secret key if we consider a real-time dynamic scenario.

C. Channel Coefficient Statistical Distribution

Another parameter that plays an important role in PhySec analysis is the statistical distribution of the channel coefficients, i.e. of the complex, normalized channel transfer functions. To generate a secure key, the legitimate channel should display a high degree of randomness. Otherwise the sequence of bits generated may result simple to be guessed. The extreme example is the one of a constant channel, where all the key

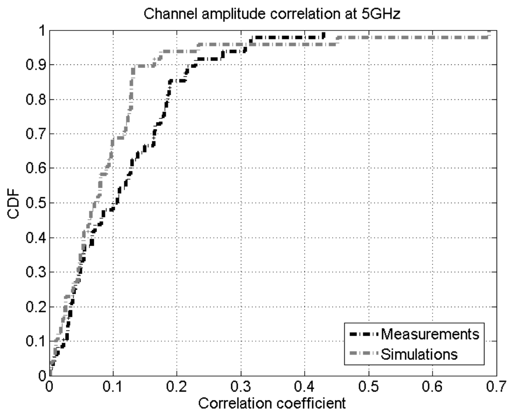

Fig. 5. CDF of correlation coefficient of channel amplitudes seen by Bob and Eve at 5 GHz

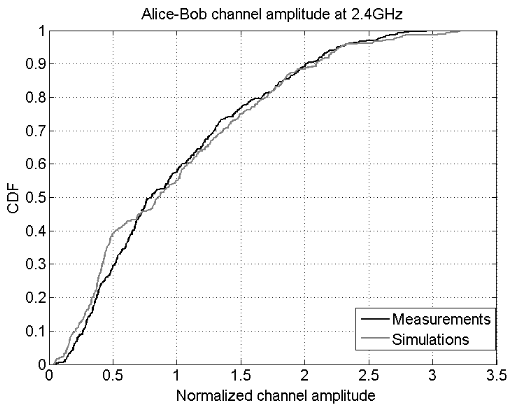

Fig. 6. Comparison of channel coefficient amplitude distribution for the three Bob positions at 2.4 GHz

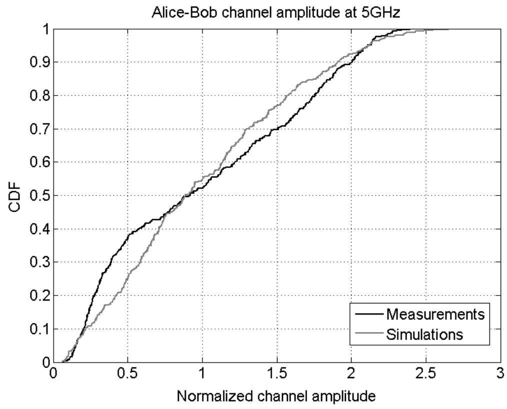

Fig. 7. Comparison of channel coefficient amplitude distribution for the three Bob positions at 5 GHz

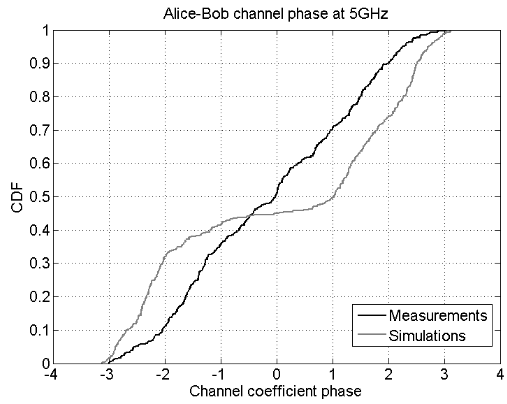

Fig. 8. Comparison of channel coefficient phase distribution for the three Bob positions at 5 GHz

bits generated would be equal to 1 (or 0). For this reason, we here investigate the capabilities of RT to reproduce the statistical distribution of the normalized channel coefficients, focusing on both their amplitude and phase. This is done for the three positions of Bob. In particular, in Fig. 6 and 7 the CDFs of the measured vs predicted channel coefficient amplitudes are reported. The agreement is satisfactory for the lower frequency, and fairly good for the upper frequency.

Fig. 8 presents the CDF of the channel coefficient phase at 5 GHz. In this case simulations significantly deviate from measurements (similar results can be found at the lower frequency). The explanation for this prediction error evidently relies in the preliminary model for the diffuse scattering phase. The uniform distribution and the lack of correlation between phases of neighboring surfaces does not model sufficiently well the phase behavior of diffuse scattering. A more realistic phase model is then required for the ER model and will be the object of future studies.

V. Conclusion

In this paper, we presented preliminary results on the evaluation of physical layer security parameters using a RT tool in an indoor environment. The Ray tracing tool, which includes the modeling of both the coherent component and the diffuse component, is validated against measurements. Two simplification hypothesis are made: a uniformly distributed random phase is associated with diffused rays and a simplified version of the input database is considered without including furniture and small objects. Preliminary results are promising as the comparison between simulations and measurements shows a very good agreement in terms of channel correlation coefficients and channel amplitude distributions. While the simplified input database doesn't seem to affect simulation accuracy, results show that a better model is required for the diffuse scattering phase distribution. Further results and a more detailed analysis of the role of diffuse scattering will be presented in future work.

Acknowledgment

This work has been carried out in the framework of COST action IC1004 on Cooperative Radio Communications for Green Smart Environments. F. Mani, T. Mazloum and A. Sibille also acknowledge the support of PHYLAWS project (EU FP7-ICT 317562, www.phylaws-ict.org).

References

[1] S. Tmar-Ben Hamida, J. Pierrot, and C. Castelluccia, "An adaptive quantization algorithm for secret key generation using radio channel measurements," in *3rd International Conference on New Technologies, Mobility and Security*, ser. NTMS '09. IEEE, 2009, pp. 1–5.

[2] J. Wallace and R. Sharma, "Automatic secret keys from reciprocal MIMO wireless channels: Measurement and analysis," *IEEE Transactions on Information Forensics and Security*, vol. 5, no. 3, pp. 381–392, Sep. 2010.

[3] C. Chen and M. Jensen, "Secret key establishment using temporally and spatially correlated wireless channel coefficients," *IEEE Transactions on Mobile Computing*, vol. 10, no. 2, pp. 205–215, Feb. 2011.

[4] F. Saez de Adana, O. Gutierrez Blanco, I. Gonzalez Diego, J. Perez Arriaga, and M. F. Cátedra, "Propagation model based on ray tracing for the design of personal communication systems in indoor environments," *IEEE Transactions on Vehicular Technology*, vol. 49, no. 6, pp. 2105–2112, 2000.

[5] C. Sturm, W. Sorgel, T. Kayser, and W. Wiesbeck, "Deterministic UWB wave propagation modeling for localization applications based on 3d ray tracing," in *Microwave Symposium Digest, 2006. IEEE MTT-S International*. IEEE, 2006, pp. 2003–2006.

[6] A. O. Kaya, W. Trappe, L. J. Greenstein, and D. Chizhik, "Predicting MIMO performance in urban microcells using ray tracing to characterize the channel," *IEEE Transactions on Wireless Communications*, vol. 11, no. 7, pp. 2402–2411, 2012.

[7] V. Degli-Esposti, V.-M. Kolmonen, E. M. Vitucci, and P. Vainikainen, "Analysis and modeling on co-and cross-polarized urban radio propagation for dual-polarized mimo wireless systems," *IEEE Trans. Antennas Propagat.*, vol. 59, no. 11, pp. 4247–4256, 2011.

[8] L. Xiao, L. Greenstein, N. Mandayam, and W. Trappe, "Using the physical layer for wireless authentication in time-variant channels," *IEEE Transactions on Wireless Communications*, vol. 7, no. 7, pp. 2571–2579, 2008.

[9] H. Ghannoum, S. Bories, C. Roblin, and A. Sibille, "Biconical antennas for intrinsic characterization of the UWB channel," in *Antenna Technology: Small Antennas and Novel Metamaterials, 2005. IWAT 2005. IEEE International Workshop on*. IEEE, 2005, pp. 101–104.

[10] V. Degli-Esposti, D. Guiducci, A. de'Marsi, P. Azzi, and F. Fuschini, "An advanced field prediction model including diffuse scattering," *IEEE Trans. Antennas Propagat.*, vol. 52, no. 7, pp. 1717–1728, 2004.

[11] V. Degli-Esposti, F. Fuschini, E. M. Vitucci, and G. Falciasecca, "Measurement and modelling of scattering from buildings," *IEEE Trans. Antennas Propagat.*, vol. 55, no. 1, pp. 143–154, Jan. 2007.

[12] F. Mani, E. M. Vitucci, F. Quitin, V. Degli-Esposti, and C. Oestges, "Parameterization of a polarimetric diffuse scattering model in indoor environments," *IEEE Trans. Antennas Propagat.*, vol. 62, no. 8, pp. 4361–4364, Aug. 2014.